Materials Research Bulletin 96 (2017) 443–448

Contents lists available at ScienceDirect

Materials Research Bulletin

journal homepage: www.elsevier.com/locate/matresbu

Hydrothermal synthesis of hollow SnO_2 spheres with excellent electrochemical performance for anodes in lithium ion batteries

Ruiping Liu[a,b,d,*], Weiming Su[a], Chao Shen[a], James Iocozzia[d], Shiqiang Zhao[d], Kunjie Yuan[d], Ning Zhang[a], Chang-an Wang[c], Zhiqun Lin[d,*]

[a] Department of Materials Science and Engineering, China University of Mining & Technology (Beijing), Beijing 100083, China
[b] State Key Laboratory of Coal Resources and Safe Mining, China University of Mining & Technology (Beijing), Beijing 100083, China
[c] School of Materials Science and Engineering, State Key Laboratory of New Ceramics and Fine Processing, Tsinghua University, Beijing 100084, China
[d] School of Materials Science and Engineering, Georgia Institute of Technology, Atlanta, GA 30332, USA

ARTICLE INFO

Article history:
Received 27 January 2017
Received in revised form 23 February 2017
Accepted 3 March 2017
Available online 6 March 2017

Keywords:
Oxides
Solvothermal
Electrochemical properties

ABSTRACT

Hollow SnO_2 spheres with oriented cone-like SnO_2 nanoparticle shells were synthesized by a one-step hydrothermal process using NaF as the morphology controlling agent. The resulting hollow SnO_2 sphere electrode exhibits high reversible capacity (initial charge and discharge capacities of 1342.9 and 1947.6 mAh/g at 0.1 C and 1235.4 and 1741.3 mAh/g at 1 C) and good cycling stability (discharge capacities maintained 758.1 and 449.6 mAh/g after 100 cycles at 0.1 C and 1 C, respectively). Good rate performance was also obtained (1234.5 mAh/g at 0.1 C, 884.2 mAh/g at 0.2 C, 692.4 mAh/g at 0.5 C, 497.6 mAh/g at 1 C, 315.8 mAh/g at 2 C and 80.6 mAh/g at 5 C, and more importantly, when the current density returns to 0.1 C, a capacity of 869.6 mAh/g can be recovered. The observed electrochemical performance can attributed to the hollow structure, the use of NaF for morphology control and the unique oriented cone-like shell of the particles.

1. Introduction

Increasing energy demands and environmental pollution are two significant problems facing modern society. One solution to these problems is using hybrid electric vehicle (HEV) and electric vehicle (EV), both of which require energy storage apparatuses with superior performance characteristics. Due to its high energy and power densities, high output voltage and long cycle life, lithium ion batteries (LIBs) have attracted much attention [1–4]. However, current commercially available lithium ion batteries limit their wider application [5–7]. It is known that the electrochemical performance of LIBs largely depends on the electrode materials. Compared to the cathode, the electrochemical properties of anode materials are likely easier to improve moving forward due to the relatively low theoretical capacity (372 mAh/g), ease of lithium dendrites formation on the electrode surface and low lithium-ion intercalation potential of commercial graphite-based anode materials. In short, there is a lot of room to improve the anode performance through novel material investigation [8–10].

Among several candidates, SnO_2 is considered a highly promising anode material for next generation LIBs due to its high theoretical capacity (782 mAh/g) and low cost [9–12]. However, poor cycling performance resulting from electrode pulverization and electrical disconnection caused by large volume changes (about 300%) during the charge and discharge process and poor rate properties resulting from the low electrical conductivity of SnO_2 have limited its development [13–15]. To address these problems, one strategy is to construct various nanostructures including nanoparticles [16,17], nanowires [18], nanofibers [19], nanotubes [20], nanosheets [21] and nanospheress [22]. Among them, hollow SnO_2 spheres are especially promising anode materials and the focus of this work. First, the hollow structure can provide space to alleviate the volume expansion during the charge/discharge processes. Second, the Li^+ diffusion distance can be shortened by controlling the shell thickness and increasing the contact area between active materials and electrolyte. Last, spheres with high density can increase both the mass energy density and volume energy density. Up to now, different methods have been used for preparing hollow SnO_2 spheres including soft template methods [23,24] and hard template methods using silica and carbon which can be removed by calcination or chemical

* Corresponding authors at: School of Materials Science and Engineering, Georgia Institute of Technology, Atlanta, GA 30332, USA.
E-mail addresses: bjlrp165@126.com (R. Liu), zhiqun.lin@mse.gatech.edu (Z. Lin).

http://dx.doi.org/10.1016/j.materresbull.2017.03.004
0025-5408/

etching [25,26]. There are drawback to both types of synthesis methods. Soft templating methods are time-consuming and complex. Whereas hard templating methods make it difficult to regulate the morphology and size of the hollow spheres.

Based on the above discussion, the hollow structures are highly beneficial for the lithium ion batteries during the charge/discharge process, and the facile synthesis methods with controllable morphology are highly desired. Herein, we report a one-step synthesis method to prepare hollow SnO_2 spheres using a hydrothermal method with improved morphology control. The electrochemical performance of the hollow SnO_2 spheres as anodes for lithium ion batteries are also investigated.

2. Experimental

2.1. Synthesis of hollow SnO_2 spheres

The hollow SnO_2 spheres were prepared using a hydrothermal method. In a typical procedure, 2 g of $SnCl_4 \cdot 5H_2O$ and 1.04 g of NaF were dispersed in 60 ml of ethylene glycol. The mixture was mixed via ultrasonication to form a homogeneous solution. The solution was transferred to a 100 ml Teflon lined stainless steel autoclave maintained at 180 °C for 24 h. After cooling to room temperature, the powder was collected and rinsed by washing with de-ionized water and ethanol (three times). The hollow SnO_2 spheres were then obtained by vacuum drying the powder at 80 °C overnight.

In order to enhance the electric conductivity of the hollow SnO_2 spheres as well as reduce the effects of volume change during the charge/discharge processes, a thin carbon layer was applied to the exterior of the particles. First, 300 mg of hollow SnO_2 spheres were dispersed in Tris solution (50 ml, pH = 8.5) for 1 h to form a uniform suspension. Next, 50 mg of dopamine hydrochloride was added to the mixture under magnetic stirring. The mixture was subjected to continuous magnetic stirring at room temperature for 12 h. The resulting SnO_2@poly-dopamine precipitated was collected by centrifugation and washed with ethanol and deionized water before being dried at 60 °C for 6 h. The resulting powder was annealed at 700 °C for 4 h under Ar to convert the poly-dopamine into carbon.

2.2. Characterization and electrochemical measurement

The morphology and phase composition of as-prepared spheres were characterized by SEM (Zeiss Supra 40 FE) and XRD (Bruker D8-Advance diffractometer). Electrochemical tests were performed using CR2032 coin-type cells assembled in a glove box (Mikrouna, Shanghai, China) filled with ultra-pure Ar. The working electrodes were produced by mixing the active material (hollow SnO_2 spheres), carbon black and polyvinylidene fluoride (PVDF) in a weight ratio of 80:10:10. Neat lithium metal foil was used as counter electrode and polypropylene (Celgard 2400) was used as a separator layer. The electrolyte was 1 M $LiPF_6$ dissolved in ethylene carbonate (EC), diethyl carbonate (DEC) and dimethyl carbonate (DMC) in a 1:1:1 vol ratio. The cells were cycled between 0.001 and 2 V (vs. Li/Li^+) at a current densities ranging from 0.1 C to 5 C at room temperature. Cyclic voltammetry (CV) was carried out on an electrochemical workstation (CHI660C, Shanghai Chenhua). The CV was performed at a scan rate of 0.1 mV/s.

3. Result and discussion

Fig. 1 shows the XRD pattern of the as-synthesized hollow SnO_2 spheres. It can be seen that the all the XRD diffraction peaks match well to the standard for SnO_2 (JCPDS: 41-1445) indicating that the as-synthesized materials are SnO_2.

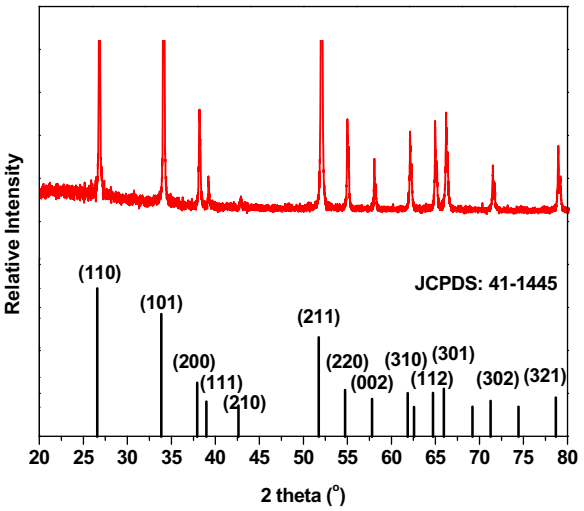

Fig. 1. XRD pattern of as-synthesized hollow SnO_2 spheres.

In order to evaluate the effects of the NaF content on the morphology of the SnO_2 spheres, the molar ratio of F/Sn was changed from 3 to 5. Fig. 2 shows SEM images of the as-synthesized hollow SnO_2 spheres with different molar ratios of F/Sn. It can be seen that when the NaF content is low, the powders are largely shapeless bulk materials (Fig. 2(a)). With increasing NaF content, the morphology of the as-synthesized powders gradually turns into spheres (Fig. 2(b–d)). When the molar ratio of F/Sn is increased to 4.77 during the hydrothermal process, a uniform distributed SnO_2 spheres with diameters of roughly 1 μm were obtained. The SnO_2 spheres bonded with each other to form chain-like structures (Fig. 2(e)) which may prove beneficial for the transportation of Li ions during charge/discharge processes. Increasing the NaF content even more led to a disappearance in the homogeneity of the microsphere shape and size (Fig. 2(f)).

Fig. 3 shows SEM images of the obtained hierarchical hollow SnO_2 spheres at the F/Sn molar ratio of 4.77 before and after the carbon coating. It can be seen that the SnO_2 spheres possess hollow interiors (Fig. 3(b)) with a rough surface. The shell is composed of oriented cone-like SnO_2 crystallites (Fig. 3(a)). It can be seen that after the carbon coating, the surface of spheres become less rough, indicating that a thin carbon layer was coated on the surface of spheres. According to previous results, fluoride ions are important for controlling the morphology and microstructure of various metal oxide structures [27]. This unique microstructure may be due to the Oswald ripening process of the original SnO_2 aggregates with the presence of NaF during the hydrothermal process. The hollow interior, cone-like shell and carbon layer may be beneficial for lithium ion and electron transportation during the charge/discharge processes.

The proposed formation mechanism of the hierarchical SnO_2 spheres is as follows (Fig. 4). First, the tin precursor undergoes fast hydrolysis to form $Sn(OH)_4$ during the hydrothermal process. This then decomposes into the primary SnO_2 crystallites with the effects of the NaF. Next, the primary SnO_2 crystallites aggregate into microspheres to reduce the surface energy. The spheres composed of randomly distributed SnO_2 crystallites are poorly crystallized due to its high surface energy. The poorly crystalized aggregates then undergo a reorganization and recrystallization process during the hydrothermal process. Lastly, the hierarchical hollow SnO_2 spheres are formed by consuming the core materials via a solid evacuation mechanism with the recrystallized shells acting as new nucleation sites [28,29].

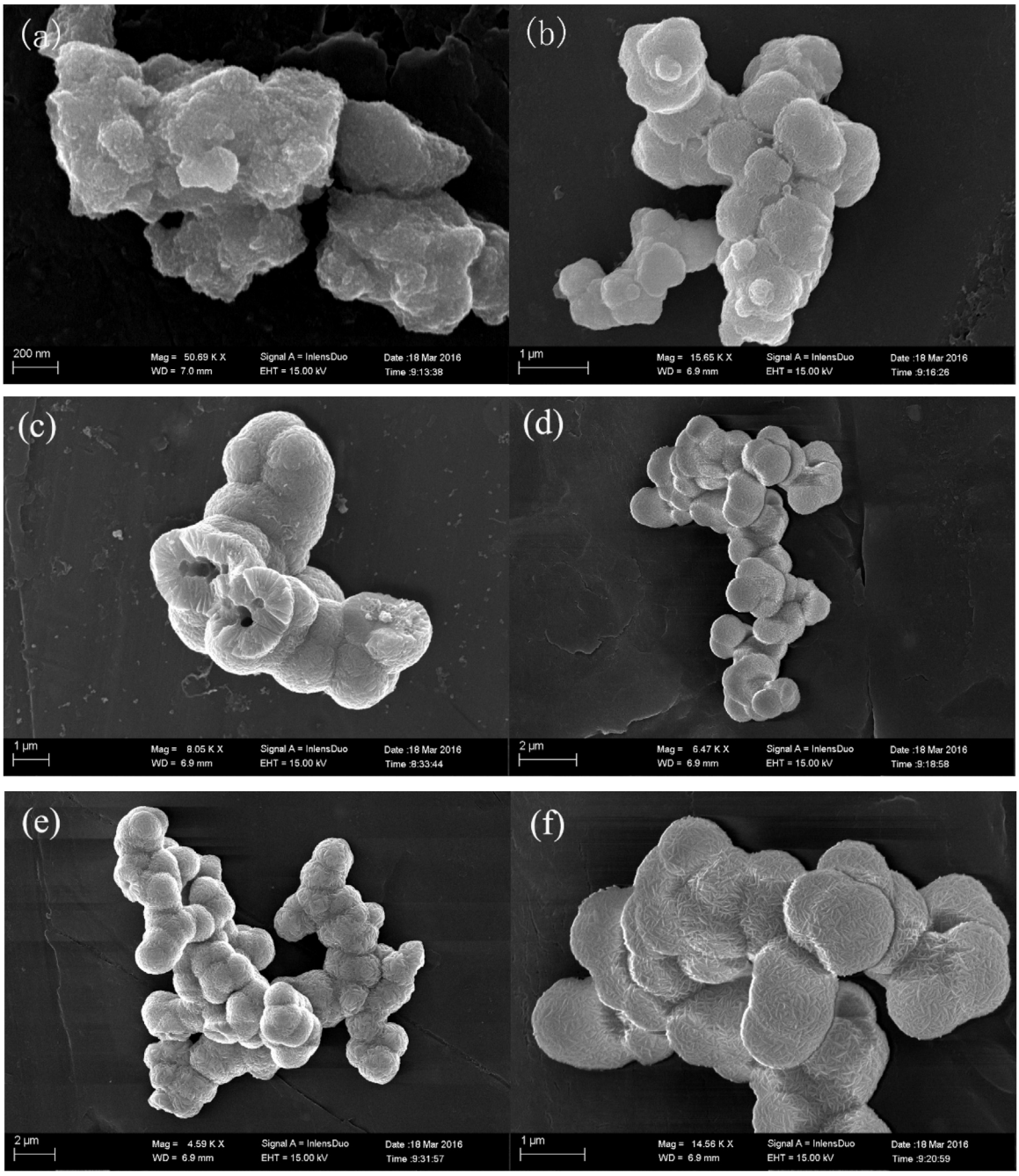

Fig. 2. SEM images of as-synthesized powders with F/Sn molar ratio of (a) 3, (b) 4, (c) 4.2, (d) 4.5, (e) 4.77 and (f) 5.

The as-synthesized hollow SnO_2 powders with a F/Sn molar ratio of 4.77 were selected for evaluation of their electrochemical performance as anode materials for lithium ion batteries. Fig. 5 shows the initial three CV curves of the carbon-coated SnO_2 hollow spheres at a scan rate of 0.1 mV/s^{-1} from 0.0 to 2.0 V. It can be clearly seen that the first charge-discharge curve is different from the others indicating irreversible reactions occurring during the process. A reduction broad peak located at 0.64 V in the first dischage process disappeared in the next two curves. This can be attributed to the formation of a solid electrolyte interface (SEI) layer on the surface of the active materials [30] and the reduction of SnO_2 to Sn and Li_2O [31]. The weak peak located at around 0.32 V can be attributed to the alloying processes between Li and Sn [32]. The sharp peak located at about 0.69 V corresponds to the reversible LixSn dealloying process. The anodic peak located at approximately 1.30 V can be assigned to the partial conversion of Sn to SnO and SnO_2. After the first cycle, the cathodic peak potential of the electrode shifts to higher voltage whereas the anodic peak shifts to lower voltage suggesting reduced anode polarization and increased Li^+ insert/extraction reversibility during electrochemical cycling.

Fig. 6 shows the cycling performance of the hollow SnO_2 powders at a current density of 0.1 C and 1 C respectively (1C = 782 mA/g) as well as the rate performance. It can be seen that the initial charge and discharge capacity of the SnO_2 spheres at a current density of 0.1 C are 1342.9 mAh/g and 1947.6 mAh/g, respectively with an initial Coulombic efficiency of 70.71%. The capacity slightly decreases to 1010.3 mAh/g in the first 10 cycles and stabilizes at 758.1 mAh/g during the subsequent remaining ninety cycles. When the current density is increased to 1 C, the

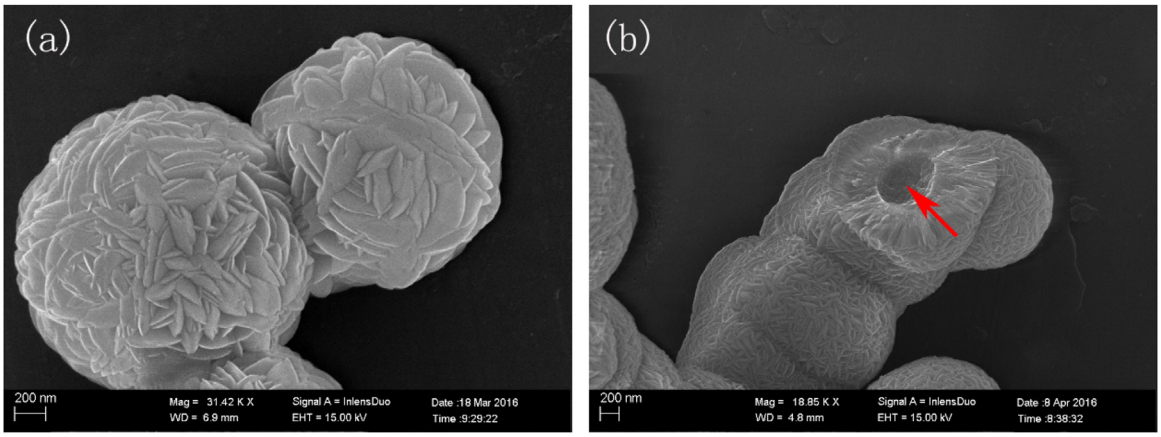

Fig. 3. SEM images of hollow SnO_2 spheres at the F/Sn molar ratio of 4.77 (a) before and (b) after the carbon coating.

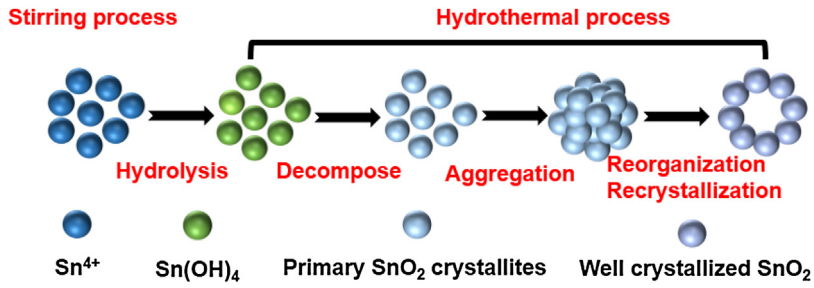

Fig. 4. Formation mechanism of hierarchical hollow SnO_2 spheres.

hollow SnO_2 spheres also show excellent electrochemical performance. In the first cycle, the electrodes deliver initial charge and discharge capacities of 1235.4 mAh/g and 1741.3 mAh/g, respectively with an initial Coulombic efficiency of 69.2%, and the capacity stabilizing at 449.6 mAh/g after the 100 charge/discharge cycles.

Fig. 6(b) shows the rate performance of the hollow SnO_2 spheres at various current rates from 0.1 C to 5 C in which the given capacity values are the average taken over 10 cycles. As expected, the capacity decreases gradually as the current rate increases. The reversible capacity of the electrode in the sixth cycle is 1234.5, 884.2, 692.4, 497.6, 315.8 and 80.6 mAh/g when cycled at 0.1 C, 0.2 C, 0.5 C, 1 C, 2 C and 5 C, respectively. Furthermore, when the current density returns to 0.1 C, a capacity of 869.6 mAh/g can be recovered. This confirms the good rate performance and stability of the hollow SnO_2 spheres.

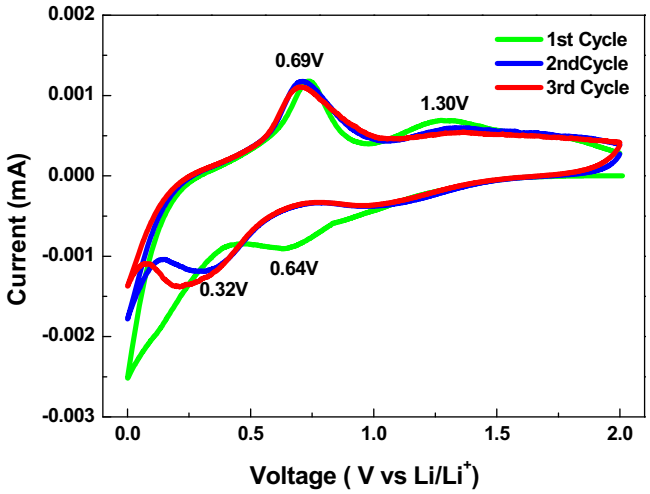

Fig. 5. Cyclic voltammetry (CV) curves of hollow SnO_2 sphere electrodes over a voltage range of 0–2 V and a scan rate of 0.1 mV/s.

Compared to hollow SnO_2 spheres synthesized by other methods, employing NaF in the hydrothermal method can improve its electrochemical properties as anode materials for lithium ion batteries. For instance, a capacity of 401 mA h/g after 50 cycles at 0.1 C was obtained for hollow spheres synthesized using carbon spheres as hard template [33], 406.5 mAh/g up to 65 cycles for hollow spheres synthesized via a facile template-free hydrothermal method combined with an annealing process [34], 545 mAh/g after 50 cycles for hierarchical SnO_2 nanostructures with hollow interiors prepared by a simple template-free route [28]. The superior lithium storage capacity can be ascribed to the unique hierarchical structure with oriented alignment of the cone-like building blocks. The introducing of fluoride ions may improve the electric conductivity of the synthesized SnO_2 spheres.

In order to further verify the differences in the electrical properties of hollow SnO_2 spheres prepared by previously-reported hard template methods and NaF-modified hydrothermal method, electrochemical impedance spectra (EIS) was performed on the hollow SnO_2 spheres. As shown in Fig. 7, the EIS spectra (Nyquist plots) are composed of a semicircle at the high-medium frequency region which can be attributed to the charge transfer reaction at the interface between the electrode and electrolyte, and an inclined line in the low frequency region corresponding to lithium-ion diffusion in the solid electrode [35]. The Nyquist plots are fitted by using the equivalent circuit model [36]. In the equivalent circuit (inset), R_s and R_{ct} are the ohmic resistance and the charge transfer resistance of the electrodes. The constant phase-angle element (CPE) and the Warburg impedance (W)

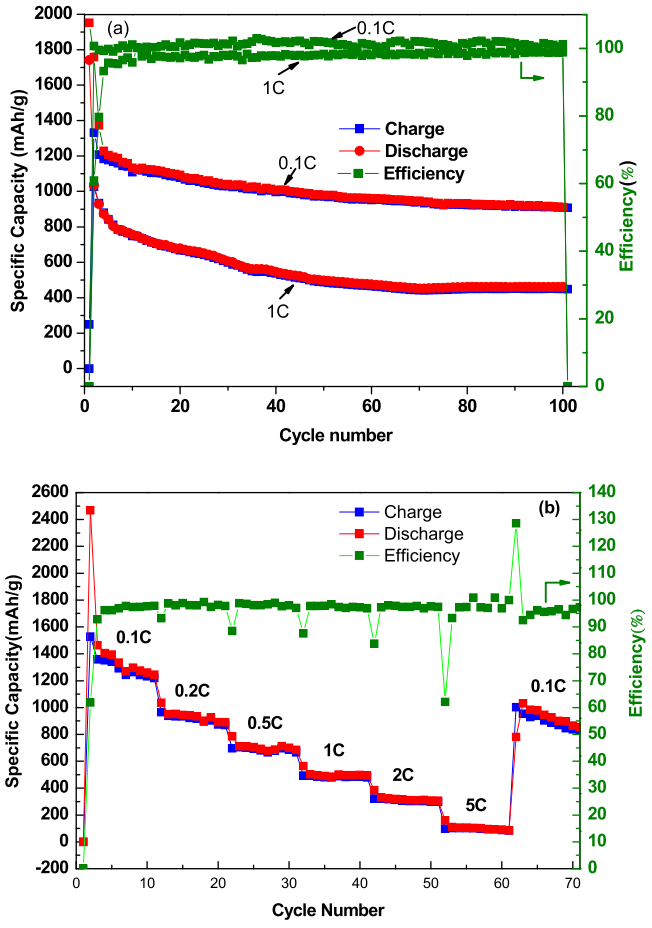

Fig. 6. (a) Cycling and (b) rate performances of hollow SnO_2 powders.

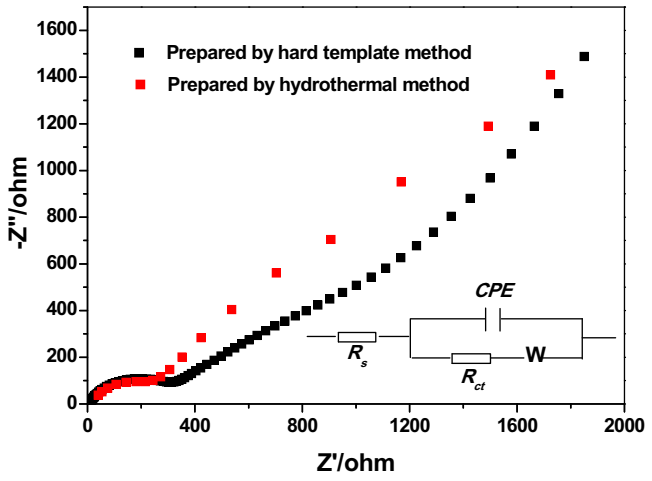

Fig. 7. EIS spectrum of hollow SnO_2 spheres prepared by NaF-modified hydrothermal method (red dots) and the previously reported hard template method (black dots [33]). (For interpretation of the references to colour in this figure legend, the reader is referred to the web version of this article.)

reflect the Li^+ diffusion into the bulk of the active materials. It can be seen that the semicircle at the high-medium frequency region of the hollow SnO_2 spheres prepared in this paper is smaller than that of previously reported hollow SnO_2 spheres with the diameter of 500–600 nm and the shell thickness of 15 nm prepared using carbon spheres as hard templates. This supports the improved electronic conductivity of the hollow SnO_2 sphere electrodes prepared in this work.

4. Conclusions

In summary, hollow SnO_2 spheres can be obtained via a one-step hydrothermal method. The addition of NaF can be used as a morphology controlling agent to regulate the microstructure of the resulting hollow SnO_2 spheres. The hollow SnO_2 spheres with diameters of 1 μm have oriented cone-like shells synthesized with a F/Sn molar ratio of 4.77 show excellent electrochemical performance as anode materials for lithium ion batteries. The poor cycling and rate performance of SnO_2 is improved by the hollow structure, fluoride doping and unique oriented cone-like shells. These results confirm that the as-prepared hollow SnO_2 spheres are a promising anode material for lithium-ion batteries.

Acknowledgments

This work was supported by the National Natural Science Foundation of China (NSFC–No. 51202117 and 51572145), Natural Science Foundation of Beijing (No. 2162037), the Beijing Nova program (Z171100001117077) and Beijing outstanding talent (No. 2015000020124G121), the Fundamental Research Funds for the Central Universities (No. 2014QJ02) and the State key laboratory of Coal Resources and Safe Mining (No. SKLCRSM16KFB04).

References

[1] Y. Li, J. Song, J. Yang, A review on structure model and energy system design of lithium-ion battery in renewable energy vehicle, Renew. Sustain. Energy Rev. 37 (2014) 627–633.
[2] B. Luo, L. Zhi, Design and construction of three dimensional graphene-based composites for lithium ion battery applications, Energy Environ. Sci. 8 (2015) 456–477.
[3] B. Huang, B. Xu, Y. Li, W. Zhou, Y. You, S. Zhong, C. Wang, John B. Goodenough, Li-ion conduction and stability of perovskite $Li_{3/8}Sr_{7/16}Hf_{1/4}Ta_{3/4}O_3$, ACS Appl. Mater. Interfaces 23 (2016) 14552–14557.
[4] J. Shao, Q. Qu, Z. Wan, T. Gao, Z. Zuo, H. Zheng, From dispersed microspheres to interconnected nanospheres: carbon-sandwiched monolayered MoS_2 as high-performance anode of Li-ion batteries, ACS Appl. Mater. Interfaces 41 (2015) 22927–22934.
[5] P. Lian, X. Zhu, S. Liang, Z. Li, W. Yang, H. Wang, Large reversible capacity of high quality graphene sheets as an anode material for lithium-ion batteries, Electrochim. Acta 55 (2010) 3909–3914.
[6] Y. Zhao, Y. Ding, Y. Li, L. Peng, H. Byon, John B. Goodenough, G. Yu, A chemistry and material perspective on lithium redox flow batteries towards high-density electrical energy storage, Chem. Soc. Rev. 44 (2015) 7968–7996.
[7] C. Wang, L. Wu, H. Wang, W. Zuo, Y. Li, J. Liu, Fabrication and shell optimization of synergistic TiO_2-MoO_3 core-shell nanowire array anode for high energy and power density lithium-ion batteries, Adv. Funct. Mater. 25 (2015) 3524–3533.
[8] I. Son, J. Park, S. Kwon, S. Park, Mark H. Rümmeli, A. Bachmatiuk, H. Song, J. Ku, J. Choi, J. Choi, S. Doo, H. Chang, Silicon carbide-free graphene growth on silicon for lithium-ion battery with high volumetric energy density, Nat. Commun. 6 (2015) 1–8.
[9] H. Wu, G. Zhang, L. Yu, X. Lou, One-dimensional metal oxide–carbon hybrid nanostructures for electrochemical energy storage, Nanoscale Horiz. 1 (2016) 27–40.
[10] Y. Li, X. Lv, J. Lu, J. Li, Preparation of SnO_2-nanocrystal/graphene-nanosheets composites and their lithium storage ability, J. Phys. Chem. C 114 (2010) 21770–21774.
[11] M. Wang, M. Lei, Z. Wang, X. Zhao, J. Xu, W. Yang, Y. Huang, X. Li, Scalable preparation of porousmicron-SnO_2/C composites as high performance anode material for lithium ion battery, J. Power Sources 309 (2016) 238–244.
[12] Z. Wang, D. Luan, F. Boey, X. Lou, Fast formation of SnO_2 nanoboxes with enhanced lithium storage capability, J. Am. Chem. Soc. 133 (2011) 4738–4741.
[13] K. Chen, T. Dong, Z. Wang, G. Li, Y. Zhang, L. Zhang, One-pot synthesis of SnO_2/C nanocapsules composites as anode materials for lithium-ion batteries, J. Nanosci. Nanotechnol. 16 (2016) 1768–1774.
[14] J. Chen, L.A. Archer, X. Lou, SnO_2 hollow structures and TiO_2 nanosheets for lithium-ion batteries, J. Mater. Chem. 21 (2011) 9912–9924.
[15] R. Sugaya, M. Sugawa, H. Nomoto, Improved electrochemical performance of SnO_2-mesoporous carbon hybrid as a negative electrode for lithium ion battery applications, Phys. Chem. Chem. Phys. 16 (2014) 6630–6640.
[16] L. Feng, Z. Xuan, S. Ji, W. Min, H. Zhao, H. Gao, Preparation of SnO_2 nanoparticle and performance as lithium-ion battery anode, Int. J. Electrochem. Sci. 10 (2015) 2370–2376.

[17] B. Jiang, Y. He, B. Li, S. Zhao, S. Wang, Y. He, Z. Lin, Polymer-templated formation of polydopamine-coated SnO_2 nanocrystals: anodes for cyclable lithium-ion batteries, Angew. Chem. Int. Ed. 56 (2017) 1869–1872.
[18] S. Seo, G. Lee, D. Kim, Three-dimensional hybrid tin oxide/carbon nanowire arrays for high-performance Li ion battery electrodes, J. Nanosci. Nanotechnol. 16 (2016) 10588–10591.
[19] W. Xie, L. Gu, F. Xia, B. Liu, X. Hou, Q. Wang, D. Liu, D. He, Fabrication of voids-involved SnO_2@C nanofibers electrodes with highly reversible Sn/SnO_2 conversion and much enhanced coulombic efficiency for lithium-ion batteries, J. Power Sources 327 (2016) 21–28.
[20] X. Sun, Y. Huang, M. Zong, H. Wu, X. Ding, Preparation of porous SnO_2/ZnO nanotubes via a single spinneret electrospinning technique as anodes for lithium ion batteries, J. Mater. Sci: Mater Electron. 27 (2016) 2682–2686.
[21] Y. Zhu, H. Guo, H. Zhai, C. Cao, Microwave-assisted and gram-scale synthesis of ultrathin SnO_2 nanosheets with enhanced lithium storage properties, ACS Appl. Mater. Interfaces 7 (2015) 2745–2753.
[22] B. Cao, D. Li, B. Hou, Y. Mo, L. Yin, Y. Chen, Synthesis of double-shell SnO_2@C hollow nanospheres as sulfur/sulfide cages for lithium–sulfur batteries, ACS Appl. Mater. Interfaces 8 (2016) 27795–27802.
[23] W. Zeng, T. Li, T. Li, J. Hao, Y. Li, Template-free synthesis of highly ethanol-response hollow SnO2 spheres using hydrothermal process, J. Mater. Sci: Mater. Electron. 26 (2015) 1192–1197.
[24] D. Li, Q. Qin, X. Duan, J. Yang, W. Guo, W. Zheng, General one-pot template-free hydrothermal method to metal oxide hollow spheres and their photocatalytic activities and lithium storage properties, ACS Appl. Mater. Interfaces 5 (2013) 9095–9100.
[25] Y. Yin, S. Li, J. Wan, C. Li, Y. Guo, SnO_2 hollow spheres: polymer bead-templated hydrothermal synthesis and their electrochemical properties for lithium storage, Sci. China Chem. 55 (2012) 1314–1318.
[26] X. Zhao, Z. Zhang, F. Yang, Y. Fu, Y. Lai, J. Li, Core–shell structured SnO_2 hollow spheres–polyaniline composite as an anode for sodium-ion batteries, RSC Adv. 5 (2015) 31465–31471.
[27] H. Wang, F. Fu, F. Zhang, H. Wang, Stephen V. Kershaw, J. Xu, S. Sun, Andrey L. Rogach, Hydrothermal synthesis of hierarchical SnO_2 microspheres for gas sensing and lithium-ion batteries applications: fluoride-mediated formation of solid and hollow structures, J. Mater. Chem. 22 (2012) 2140–2148.
[28] M. Yin, C. Li, M. Zhang, One-step synthesis of hierarchical SnO_2 hollow nanostructures via self-assembly for high power lithium ion batteries, J. Phys. Chem. C 114 (2010) 8084–8088.
[29] C. Han, D. Yang, Y. Yang, B. Jiang, Y. He, M. Wang, A. Song, Y. He, B. Li, Z. Lin, Hollow titanium dioxide spheres as anode material for lithium ion battery with largely improved rate stability and cycle performance by suppressing the formation of solid electrolyte interface layer, J. Mater. Chem. A 3 (2015) 13340–13349.
[30] X. Chai, C. Shi, E. Liu, Hierarchically structured carbon-coated SnO_2-Fe_3O_4 microparticles with enhanced lithium storage performance, Appl. Surf. Sci. 361 (2016) 1–10.
[31] P. Lian, J. Wang, D. Cai, L. Ding, Q. Jia, H. Wang, Porous SnO_2@C/graphene nanocomposite with 3D carbon conductive network as a superior anode material for lithium-ion batteries, Electrochim. Acta 116 (2014) 103–110.
[32] J. Chen, X. Lou, SnO_2 -based nanomaterials: synthesis and application in lithium-ion batteries, Small 9 (2013) 1877–1893.
[33] R. Liu, W. Su, P. He, C. Shen, C. Zhang, F. Su, C. Wang, Synthesis of SnO_2/Sn hybrid hollow spheres as high performance anode materials for lithium ion battery, J. Alloy Compd. 688 (2016) 908–913.
[34] R. Liu, N. Li, D. Li, G. Xia, Y. Zhu, S. Yu, C. Wang, Template-free synthesis of SnO_2 hollow microspheres as anode material for lithium-ion battery, Mater. Lett. 73 (2012) 1–3.
[35] K. Xie, M. Guo, W. Lu, H. Huang, Aligned TiO_2 nanotube/nanoparticle heterostructures with enhanced electrochemical performance as three-dimensional anode for lithium-ion microbatteries, Nanotechnology 25 (2014) (455401-455401).
[36] T. Xia, W. Zhang, Z. Wang, Y. Zhang, X. Song, J. Murowchick, V. Battaglia, G. Liu, X. Chen, Amorphous carbon-coated TiO_2 nanocrystals for improved lithium-ion battery and photocatalytic performance, Nano Energy 6 (2014) 109–118.